CHARACTERISTICS OF THE NEAR WAKE OF AIRFOIL SECTIONS

M.S. Mohamed, M.A. Rayan and S.G. El-Sarraf
Mechanical Power Engineering Department, Faculty of Engineering, Mansoura University.
El-Nasr Comp. for Fertilizers and Chemical Industries

خواص منطقة التضاعف القريبة من الاسطح الانسيابية الحاملة

الخلاصة:

يقدم هذا البحث دراسة تجريبية للانسياب المضطرب لمنطقة التضاعف التي تحدث مباشرة خلف الحافة الخلفية للاسطح الانسيابية الحاملة. ويعتبر هذا النوع من الانسياب ذات أهمية عملية للآلات التربينية (خاصة تصميم ريش التربينات والضواغط) وكذلك في صناعة الطائرات. استخدم في هذه الدراسة جهاز قياس سرعة الهواء بواسطة السلك الساخن حيث تم قياس قيم السرعة المتوسطة والسرعة الترددية عند مقاطع مختلفة داخل الانسياب باستخدام سلك ساخن مفرد بينما استخدم السلك الساخن المزدوج لقياس اجهاد القص عند نفس المقاطع. استخدم نوعان من الاسطح الانسيابية الحاملة هما (NACA 0012 & NACA 2415) عند أربعة زوايا انسياب مختلفة لبيان تأثير اختلاف شكل السطح وزوايا الانسياب على شكل السريان. ثلاثة سرعات سريان مختلفة استخدمت لبيان تأثير تغير رقم رينولدز على شكل السريان. قد بينت الدراسة أن زيادة رقم رينولدز يؤدي الى تكون منطقة تضاعف أقل عرضا مع وجود دوامات عالقة بالسريان بينما زيادة زاوية الانسياب يزيد من عرض منطقة التضاعف. كما بينت أن شكل سطح الانسياب يؤثر على شكل منطقة التضاعف و طريقة نموها في اتجاه السريان. تعتبر هذه الدراسة التفصيلية دليلا جيدا لفهم هذا النوع من السريان كما يمكن استخدام هذه النتائج كدليل لتطوير نماذج الاضطراب الرياضية المستخدمة للتنبئ بهذا النوع من الانسياب.

ABSTRACT:

This paper presents an experimental investigation to the near wake turbulent flow that occurs immediately behind the trailing edge of airfoil sections. The flow is of practical importance for both turbomachinery applications (turbine and compressor blades' design) and aircraft industry. Hot wire anemometry was employed in this study to measure the longitudinal mean velocity profiles U, longitudinal fluctuating velocity profiles $\sqrt{\overline{u^2}}$ and shear stress profiles $\overline{uv}$ using both single and double wire probes. Two airfoil sections (NACA 0012 and NACA 2415) at different angles of attack ($\alpha = 0^o, 2^o, 4^o$ and -2^o), on the development of the wake in the downstream distance. Three sets of free stream velocities (10, 30 and 50 m/s) were used to show the influence of Reynolds number on the flow pattern. The results show that as Reyonlds number increases, the wake becomes narrower with vortices along the flow, while the increase of the angle of attack increases the wake width. It also indicated that the shape of the airfoil section affects the wake shape and its decay in the downstream distance. These detailed results provide a good guidance of understanding this flow.

1.INTRODUCTION:

The free turbulent mixing layer is of fundamental importance in fluid mechanics. This subject is also of considerable importance in aeronautical engineering, since the wakes behind aircraft and turbine blades involve turbulent mixing. Because of the complexity of the problem, and for the sake of convenience, the free mixing layer is categorized into two regimes, namely the near wake and the far wake. In the far wake, the flow is dominated by large-scale turbulent structures and has well-established equilibrium characteristics. On the other hand, the flow in the near wake is far for equilibrium. In this region, the oncoming boundary layer (which is rich in shear) is rapidly transformed into a free shear layer.

Fukano et al [1-2] have investigated experimentally the characteristics of the wake of a rotating flat plate with a large angle of attack with special attention on the flow near the tip of the plate. They found that when the tip clearance is small, the dead air region becomes large towards the tip of the plate and the shear layer of the suction side of the plate curves outward as a result of the accumulation of low-energy fluid. On the other hand, when the tip clearance is large, the leakage flow is so large that the leakage vortex is generated from the trailing edge of the suction side and shear layer forms by contacting the leakage flow and the dead air region. The variation of the flow rate and the momentum of the wake flow are closely related to those of the leakage flow.

Hanson and Patrick [3] studied the flow in the wake of a model single rotating profan rotating in a wind tunnel using a hot-wire anemometer system designed to determine the three periodic velocity components. They used special data acquisition and data reduction methods to deal with high data frequency, narrow wakes and large fluctuating air angles in the tip-vortex region. They also investigated the flow theoretically using a simple analytical wake theory to identify the flow features such as viscous velocity defects, vortex sheets, tip vortices and propagation acoustic pulses.

Sirka et al [4] measured the values of U, V and u, v in the region of the near wake of a circular cylinder in crossflow. They noticed from the distribution of the average velocities in the wake that a zone with large velocity gradient plus a separation zone exists in the immediate vicinity of the cylinder. The measured average velocity distributions on the axis of the wake show that the separated flow in the wake region merges at x/d equals 1.3.

Some investigations were made to study and predict turbulent wake flow [5-8]. However, there is still no definite way which would lead to a method for predicting correctly all the flow parameters. Therefore, experimental techniques are being continuously refined and numerical techniques are being improved in order to achieve a general turbulence model which is able to predict this kind of flow. The key point lies in detailed, precise experiments whose results are sure to aid in analysis of the structure of wake flow. Such data are needed for

checking analytical models. This experimental investigation provides experimental data that is needed for developing and testing turbulence models for wake flow specially in the near wake region. It is rather complicated than the far wake region where the flow transforms its self from boundary layer flow to wake flow.

2. TEST RIG AND MEASURING EQUIPMENTS:

The wind tunnel employed in this experiment was of the open-circuit type, shown in figure (1). The main tunnel air was supplied to the test section at a maximum air velocity of approximately 55 m/s with free stream turbulence intensity [$\sqrt{\overline{u^2}}$ / U] less than 0.5 %. The control panel of the wind tunnel consists of a variable frequency controller and a remote speed control device. The air speed in the test section can be controlled from the control panel of the wind tunnel using a precalibrated curve.

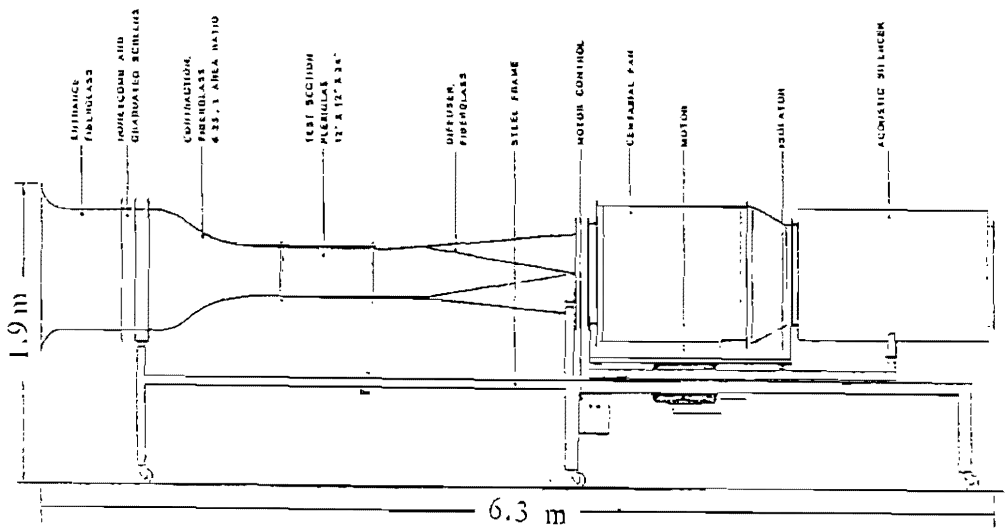

Figure (1) Open circuit wind tunnel.

The test section, which is made of perspex, has a square cross-section 305 X 305 mm and 610 mm long, figure (2-a). At the top wall of the test section, a traversing unit was fixed and a small slot in the longitudinal direction was made to accommodate the probe holder. A102 mm diameter access port is provided in the front sidewall. The port is closed during operation by a flanged plexiglas plug. A degree indexed scaled surrounds the port to allow the airfoil to be inclined with the desired angle of attack. Two stainless steel thumb screws are used to secure the plug in the port. Two NACA airfoil sections were used in this investigation, namely, NACA 0012 and NACA 2415 both of them are 100 mm cord, figure (2-b).

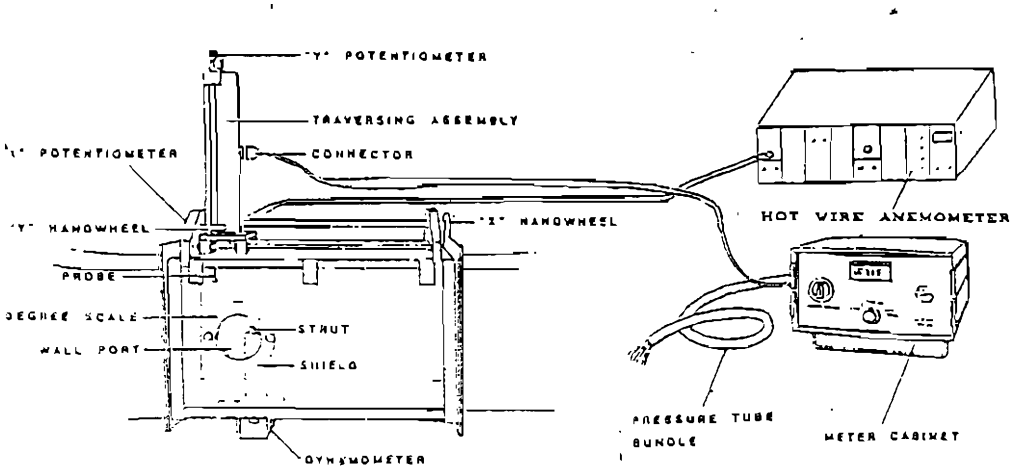

Figure (2-a) Instrumentation system components.

NACA 0012 NACA 2415

Figure(2-b) Airfoil sections employed.

2.1.METER CABINET:

The cabinet meter was used in this study to measure the pressure and the longitudinal and traverse coordinates of the probe, figure (2). On the front panel, There is a mode selector switch, a pressure selector valve and digital display to readout the selected signal. On the back panel, signal cable and pressure tube connectors are arrayed. The six operation modes are switch selectable and displayed on the digital panel meter in the selected engineering units.

2.2.PROBE TRAVERSING UNIT:

The probe traversing unit employed in this experiment has two axes traversing mechanism that is capable of positioning and reporting the location of the probe at any point in the test section vertical centerline plane, figure (2). The device is driven manually via two handwheels precise and high helix aluminum lead screws running in polyurethane nuts. Two precision potentiometers are

secured to the drive screws to report the location of the probe in each axis. The voltage signal from each potentiometer is transmitted to the digital display in the cabinet meter. The probe can be traversed from the floor to the ceiling of the test section.

2.3.HOT WIRE ANEMOMETERY:

The hot wire anemometer is an instrument extensively used to analyses in space and time the velocity fluctuations in turbulent flows. Its usefulness for making fluctuating measurements is well known [9]. Its detecting element is an active length of a small diameter wire that has a short response time, sufficient sensitivity and gives little disturbance to the flow.

Two types of hot wire probes were employed in this study. Single hot wire probes DANTEC type 55P11 are used in measuring the longitudinal mean and fluctuating velocities ($\overline{U}$, $\sqrt{\overline{u^2}}$). Cross hot wire probes, DANTEC type 55P51, were employed to measure the traversing mean velocity $\overline{V}$ and the shear stress in the flow field $\overline{uv}$.

Two DANTEC type 56C17 constant temperature anemometers (CTA) were used. One anemometer was employed with the single hot wire probe measurements, while the two anemometers were used simultaneously when using the cross wire probes. Two DANTEC 55N21 linearizers were used, one for each anemometer probe combination. After setting the anemometer and the linearizer according to the relevant instruction manuals, a calibration to the wires was made to obtain the linearizers constants.

A DANTEC 56N23 Analog Processor Unit (APU) was employed with the cross hot wire measurements. The analog processor unit allows the measurement of the instantaneous sums and ditferences of the two output signals coming from the anemometer-linearizer combinations. These sums and differences were used to resolve the instantaneous U(t) and V(t) components which can, in turn, be used to compute the shear stress and the traversing mean velocity component $\overline{V}$ in the flow field.

A DANTEC 56N22 mean value unit was used to record the mean value of the signal which is coming from the linearizer or the analog processor unit (APU). A selecting knob is used to specify which device is in connection with the mean value unit. Also, A DANTEC 56N25 root mean square RMS unit is employed to read out the fluctuating component of the signals.

3.EXPERIMENTAL PROCEDURE:

Calibration for the wind tunnel air speed against the frequency of the wind tunnel variable frequency controller was made using a pitot tube and the pressure transducer. The pressure was converted into speed and a straight line relation between the air speed and the frequency was obtained.

Calibrations for the single hot wire probe and for each wire of the two wires of the cross hot wire probe were made in the wind tunnel. The linearized signals (volts) were plotted against the air velocity to obtain the wires constants. For each calibration, it was checked that a straight line was obtained with an accuracy better than 1%. Calibrations were checked after each test-run and the average value for each wire was used in processing the signals. Calibration drifts due to various reasons were found to be small, being less than ∓5%.

Single hot wire probe was used in measuring the mean longitudinal velocity U and the fluctuating velocity component $\sqrt{\overline{u^2}}$. According to analysis of the velocity components affecting the single hot wire made by M. S. Mohamed [10], these parameters have the expressions:

$$\overline{E}_L = C\overline{U} \qquad \text{and} \qquad \sqrt{\overline{e_L^2}} = C\sqrt{\overline{u^2}} \quad \ldots\ldots (1)$$

where C is the single hot wire constant obtained from the calibration curve for that wire.

The mean voltage value $\overline{E}_L$ can be obtained from the DANTEC 56N22 mean value unit while the fluctuating voltage $\sqrt{\overline{e_L^2}}$ can be obtained from the DANTEC 56P25 RMS unit. Sampling rate can be selected for the mean value unit and the RMS unit according to the level of turbulence intensity in the flow.

The cross hot wire probe was employed to resolve the two instantaneous velocities U(t) and V(t) in order to determine the longitudinal mean velocity component U , the traversing mean velocity component V and the shear stress $\overline{uv}$. These quantities were found to have the values [10]:

$$\overline{U} = \frac{1}{\sqrt{2}} \left[\frac{\overline{E}_1}{C_1} - \frac{\overline{E}_2}{C_2} \right] \quad \ldots\ldots (2)$$

$$\overline{V} = \frac{1}{\sqrt{2}} \left[\frac{\overline{E}_1}{C_1} - \frac{\overline{E}_2}{C_2} \right] \quad \ldots\ldots (3)$$

$$\overline{uv} = \frac{1}{2}\left[\frac{\bar{e}_1^2}{C_1^2} - \frac{\bar{e}_2^2}{C_2^2}\right] \qquad \ldots\ldots\ldots (4)$$

where C_1 and C_2 are the two wires constants obtained from the calibration procedure.

Equations (2), (3) and (4) were solved numerically using the linearized signals coming from the two wires of the cross hot wire probe as input to the solution.

After calibrations were made, the employed airfoil was fixed in the test section with the required angle of attack. The probe and probe holder were mounted in the traversing unit at the required downstream distance. The frequency of the variable frequency controller of the wind tunnel was adjusted to give the required air speed in the test section according to the calibration curve. At every downstream section (x axis), the probe was driven manually (by the y-handwheel of the traversing unit) in the vertical direction (y axis) in steps varying between 0.1 mm and 5 mm according to the local mean velocity gradient and local turbulence intensity. At the end of each test run, the probe was driven manually (via the x-handwheel of the traversing unit) to the selected new downstream section and the same proceeding was made as mentioned above.

Three sets of air speeds were used in order to indicate the effect of Reynolds number on the results. These velocities are 10, 30 and 50 m/s. Two different airfoils (NACA 0012 and NACA 2415) were employed to show the effect of the body shape on the wake development in the downstream distance. Also, the angle of attack was changed to indicate its effect on the flow field. Four sets of angle of attack were used, namely, ($\alpha = 0^o, 2^o, 4^o$ and -2^o) . Two types of hot wire anemometers were used to have different data. The single hot wire was employed to obtain the longitudinal mean velocity U and the fluctuating velocity component $\sqrt{\overline{u^2}}$, while the cross hot wire anemometer was used to obtain the shear stress $\overline{uv}$ distribution in the flow field. These measurements were carried out at five different downstream sections, namely, x/c = 0.02, 0.2, 0.83, 1.8 and 3.0 where c is the airfoil cord distance.

4.RESULTS:

The experimental results obtained in this investigation were too large to be represented in this paper. Only selective samples of the results were chosen to explain the phenomena.

For airfoil section NACA 0012, the three external mean velocity values (U = 10, 30, and 50 m/s) at only one angle of attack $\alpha = 0^o$ was represented in figures (3-14). Figures (3, 6 and 9) show the absolute value for the longitudinal mean

velocity profiles U. The longitudinal fluctuating velocity profiles $\sqrt{\overline{u^2}}$ and the shear stress profiles $\overline{uv}$ versus the transverse distance y at five downstream distances (x/c =0.02, 0.2, 0.83, 1.8 and 3.0) for the above three external velocities were also shown in figures (3, 6 and 9). Figures (4, 7 and 10) represent the dimensionless longitudinal mean velocity profiles $(U-U_\varepsilon)/U_o$, the dimensionless longitudinal fluctuating velocity profiles $\sqrt{\overline{u^2}}/U_o$ and the dimensionless shear stress profiles $\overline{uv}/U_o^2$ versus the dimensionless transverse distance $y/Y_{1/2}$ at the five downstream distances. The curves were normalized with respect to the characteristic velocity $(U_o = U - U_{min})$ and the characteristic length $Y_{1/2}$, (where $Y_{1/2}$ is the distance from the center-line to the location where the velocity is half the external velocity). Figures (5, 8 and 11) represent the variation of the wake half-width ($Y_{1/2}/c$), the variation of the minimum longitudinal mean velocity $(U-U_\varepsilon)/U_o$, the variation of the maximum longitudinal fluctuating velocity $\sqrt{\overline{u^2_{max}}}/U_o$ and the variation of the dimensionless maximum shear stress ($\overline{uv}/U_o^2$) with the downstream distance x/c for the above three external velocities.

For airfoil section NACA 2415, the curves that represent the general behavior of the wake for the above three external velocities (10, 30 and 50 m/s) were selected. Figures (12, 13 and 14) represent the variation of the wake half-width ($Y_{1/2}/c$) the downstream distance x/c. The variation of the excess longitudinal mean velocity $(U-U_\varepsilon)/U_o$ versus x/c, also, is shown in these figures. The variation of the maximum longitudinal fluctuating velocity, $\sqrt{\overline{u^2_{max}}}/U_o$, with the downstream distance x/c is presented in figures (12, 13 and 14). They also include the variation of the dimensionless maximum shear stress $\overline{uv}/U_o^2$ with the downstream distance x/c.

The results show that the wake spreads in the downstream direction, therefore the minimum longitudinal mean velocity U_{min} increases. The rate of increase depends on the Reynolds number. It increases with the increase of Reynolds number. The width of the wake was found to be reduced with the increase of Reynolds number and the decrease of the angle of attack, figures (5-a, 8-a and 11-a). The center-line fluctuating longitudinal velocity $\sqrt{\overline{u^2_{max}}}$ reduces as the wake spreads in the downstream distance. The dimensionless fluctuating longitudinal velocity $\sqrt{\overline{u^2_{max}}}/U_o$ increases with the increase of Reynolds number while it decreases with the increase of angle of attack. The results, also, indicated that the shear stress decays with the downstream distance x since the velocity gradient decreases. The dimensionless shear stress $\overline{uv}/U_o$ profiles show that it

decreases with the increase of the angle of attack while it decreases with the increase of Reynolds number.

5.DISCUSSION:

The results show that, the size of the wake and its length depends on the free stream Reynolds number, the shape of the airfoil section and the angle of attack. In the following section, the effect of each parameter on the flow pattern is discussed.

5.1.EFFECT OF AIRFOIL GEOMETRY:

In almost all cases in which flow takes place round a solid body, the boundary layer separates from the surface towards the rear of the body. Downstream of the separated position, the flow is greatly disturbed by large scale eddies, and this region of eddying motion is usually known as the wake. As a result of the energy dissipated by the high intensity vortices in the wake, the pressure there is reduced and the entrainment rate of the external flow to the wake is increased. The results show the magnitude of entrainment depends very much on the size of the wake and this, in turn, depends on the position of separation.

For airfoil section NACA 0012 (streamlined body), the shape of the body is such that separation occurs only towards the rear, and the wake is small, figure (4-a). Therefore, the rate of entrainment is small and the rate of increase of minimum velocity U_{min} is small that is obvious from the slope of the curves represent the variation of the minimum longitudinal mean velocity, $(U-U_E)/U_o$, with the downstream distance, x/c, figure (4-b). For airfoil section NACA 2415, on the other hand, the flow is separated much faster than airfoil NACA 0012 and the wake is large, figure (11-a), which makes the rate of increase of minimum velocity much higher as shown in figure (11-b).

5.2.EFFECT OF REYNOLDS NUMBER:

The results indicated that the flow pattern in the wake depends on the Reynolds number ($R_e = Uc/\upsilon$) of the flow. For airfoil NACA 0012 at lower Reynolds number ($R_e = 2.667 \times 10^4$) figure (3-a), the longitudinal mean velocity profiles indicated that, at outer edges of the wake, the mean velocity was slightly less than 10 m/s in the first three downstream sections (x/c = 0.02, 0.2 and 0.83) while it reaches its maximum value (U =10 m/s) in the last two sections. In this case, the boundary layer separates symmetrically from the two sides of the airfoil and two eddies are formed which rotate in opposite directions. They remain unchanged in position, their energy being maintained by the flow from the separated boundary layer, figure (15-a). Behind the eddies, however, the

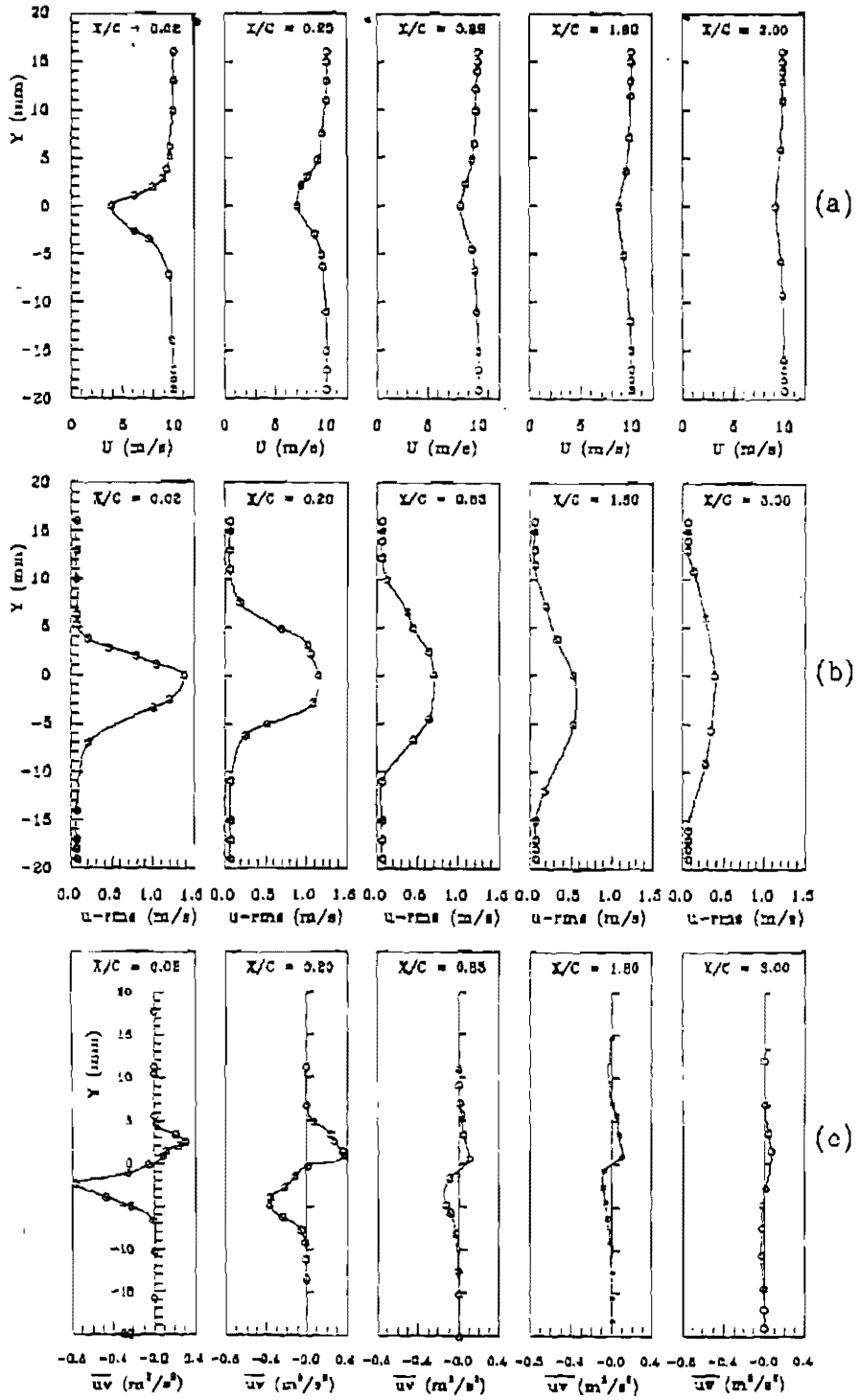

Figure (3) Wake parameters for NACA 0012 at U = 10 (m/s) and α = 0°.
a) Longitudinal mean velocity. b) Longitudinal fluctuating velocity.
c) Shear stress.

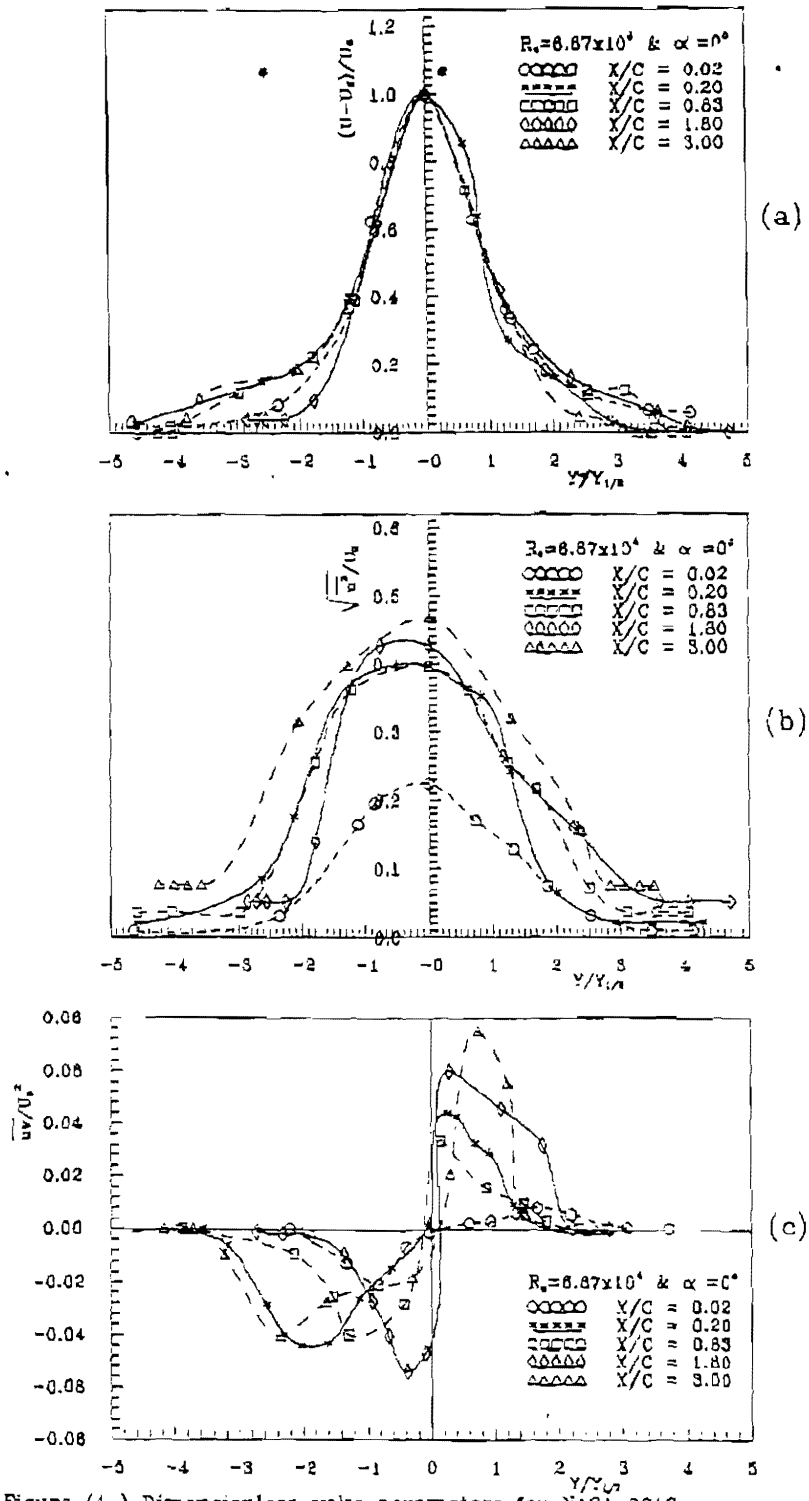

Figure (4) Dimensionless wake parameters for NACA 0012.
a) Longitudinal mean velocity. b) Longitudinal fluctuating velocity.
c) Shear stress.

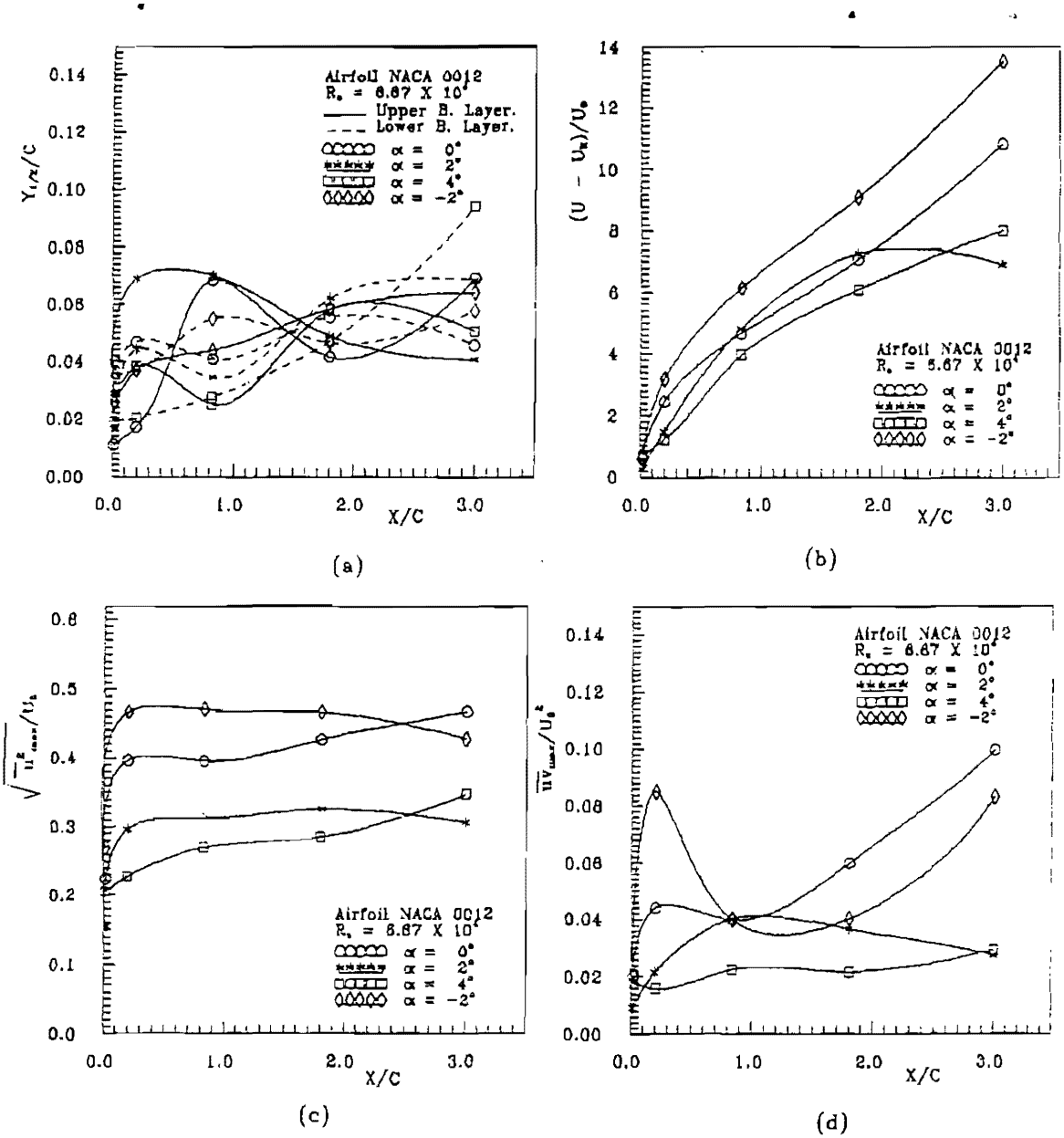

Figure(5) Variation of wake characteristics with downstream distance for NACA 0012
a) Wake half-width. b) Minimum longitudnal mean velocity.
c) Maximum longit. fluctuating velocity. d) Shear stress.

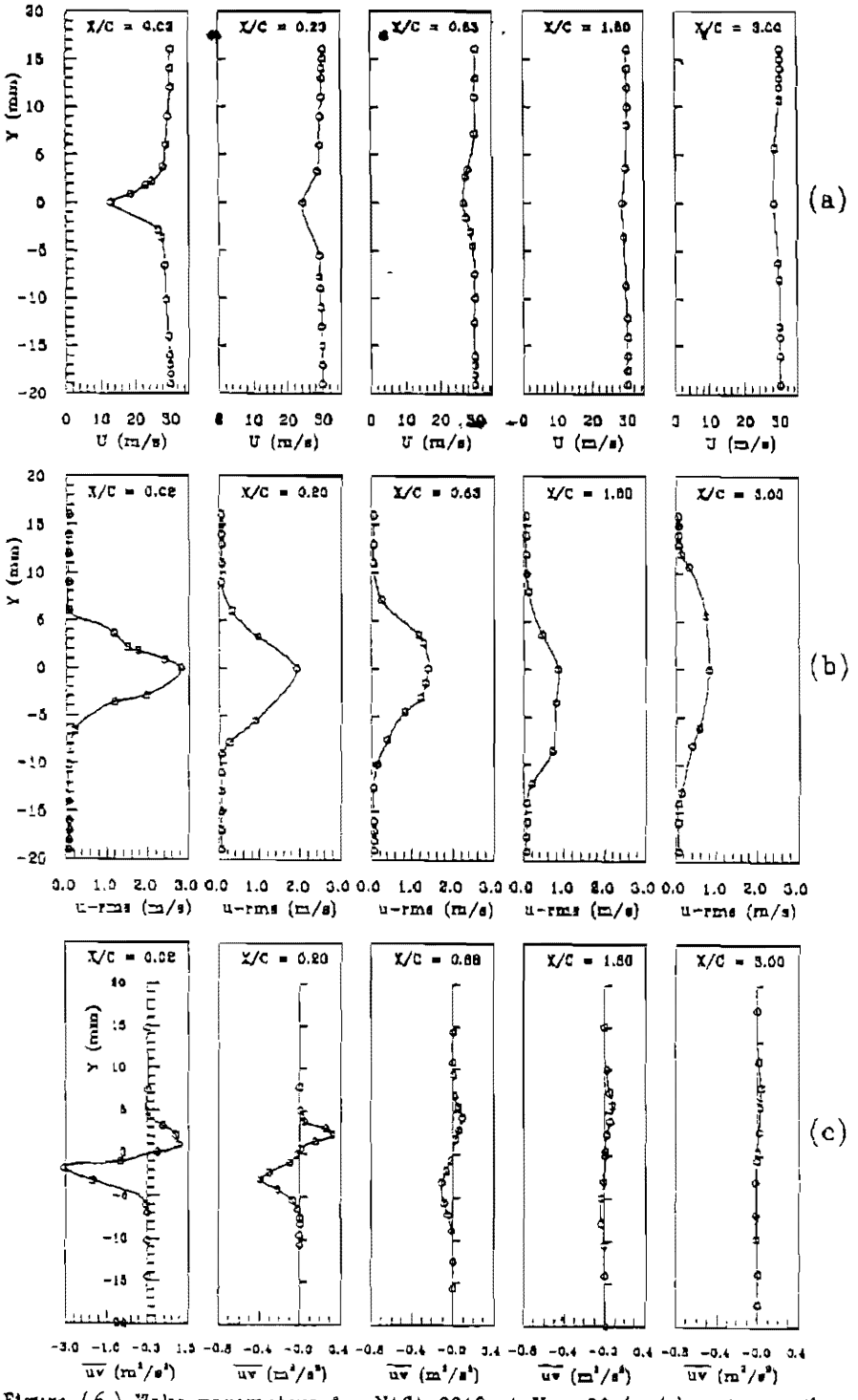

Figure (6) Wake parameters for NACA 0012 at U = 30 (m/s) and α = 0°.
a) Longitudinal mean velocity. b) Longitudinal fluctuating velocity.
c) Shear stress.

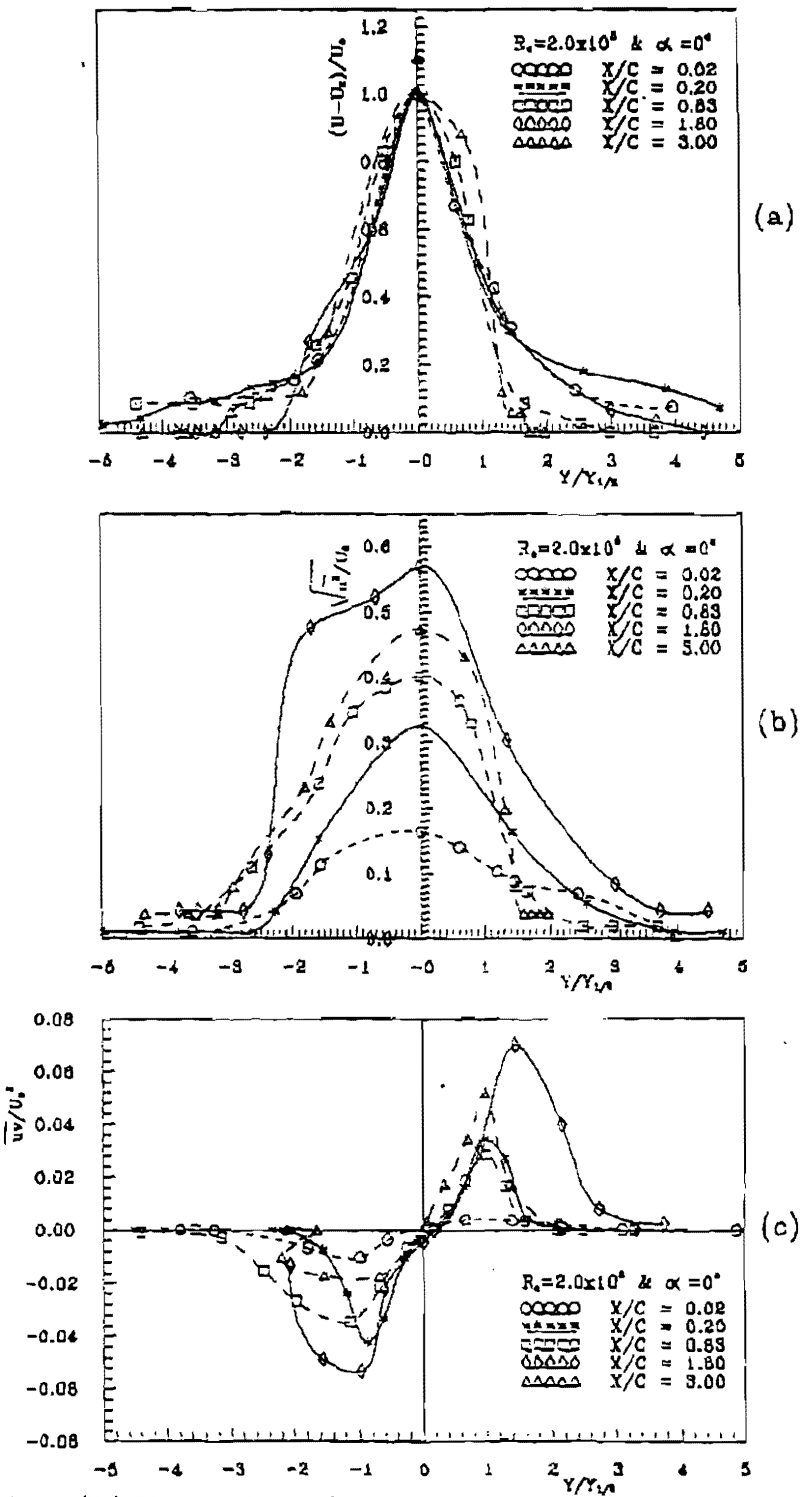

Figure (7) Dimensionless wake parameters for NACA 0012.
a) Longitudinal mean velocity. b) Longitudinal fluctuating velocity.
c) Shear stress.

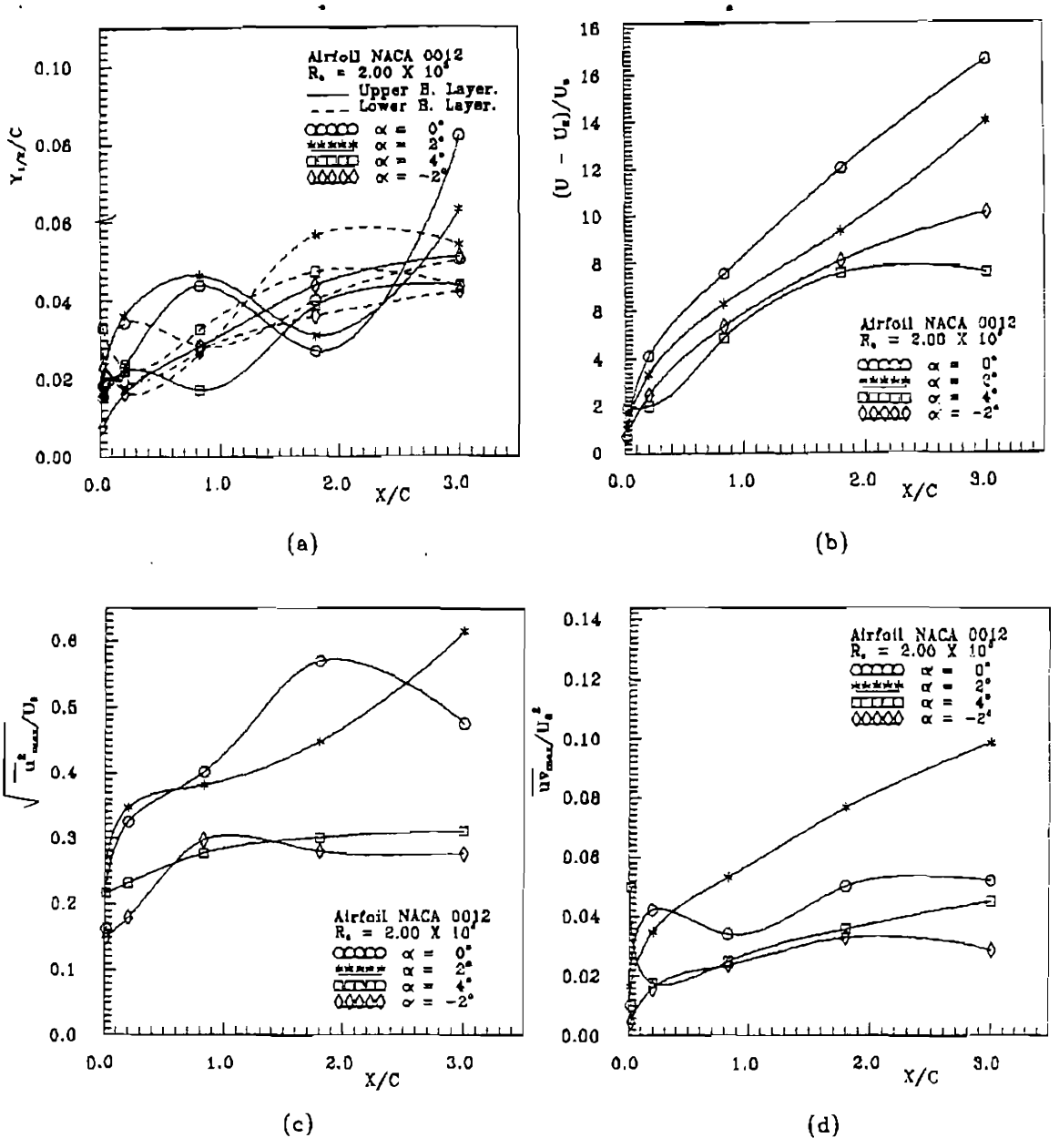

Figure(8) Variation of wake characteristics with downstream distance for NACA 0012
a) Wake half-width. b) Minimum longitudnal mean velocity.
c) Maximum longit. fluctuating velocity. d) Shear stress.

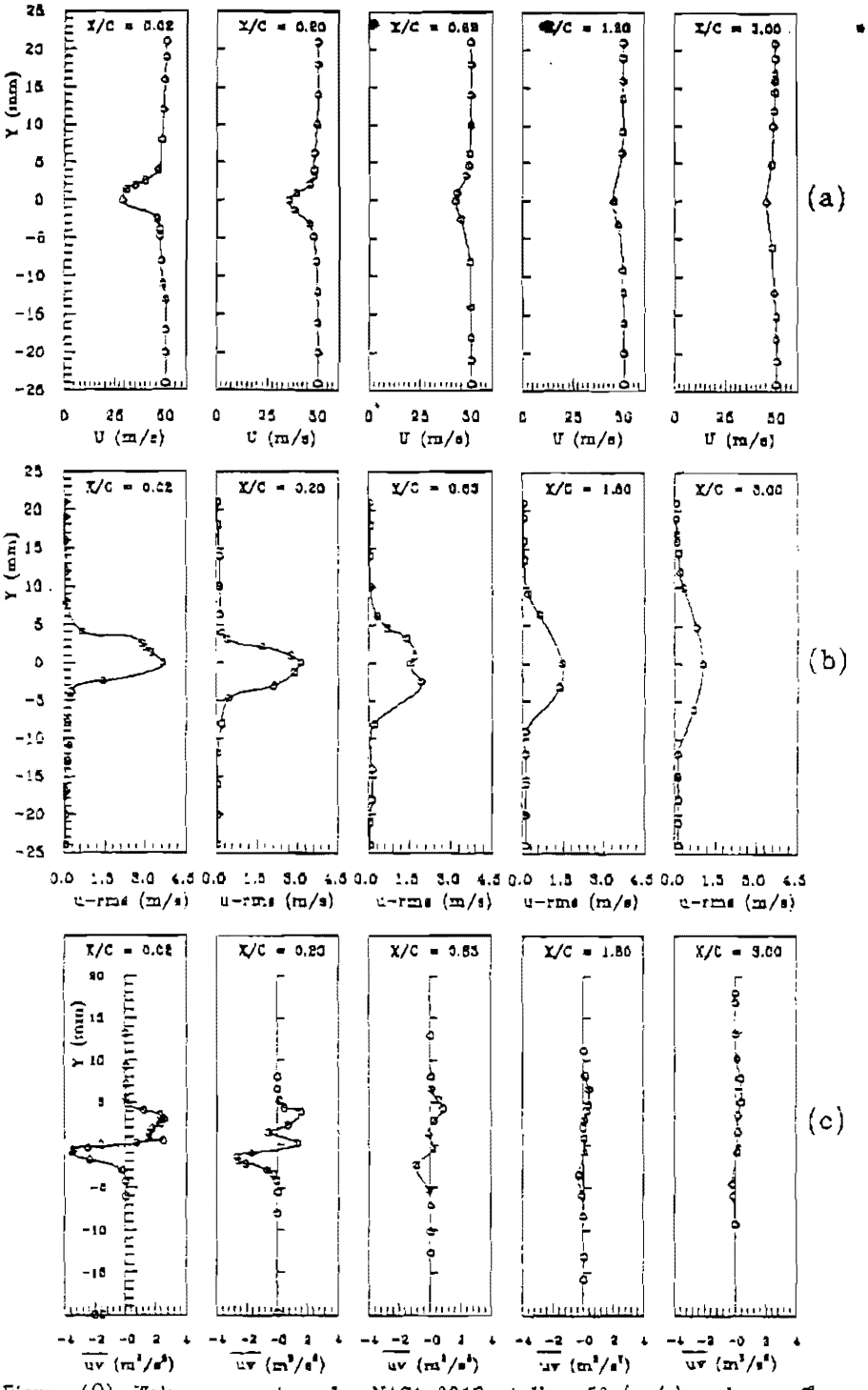

Figure (9) Wake parameters for NACA 0012 at U = 50 (m/s) and $\alpha = 0^{\circ}$.
a) Longitudinal mean velocity. b) Longitudinal fluctuating velocity.
c) Shear stress

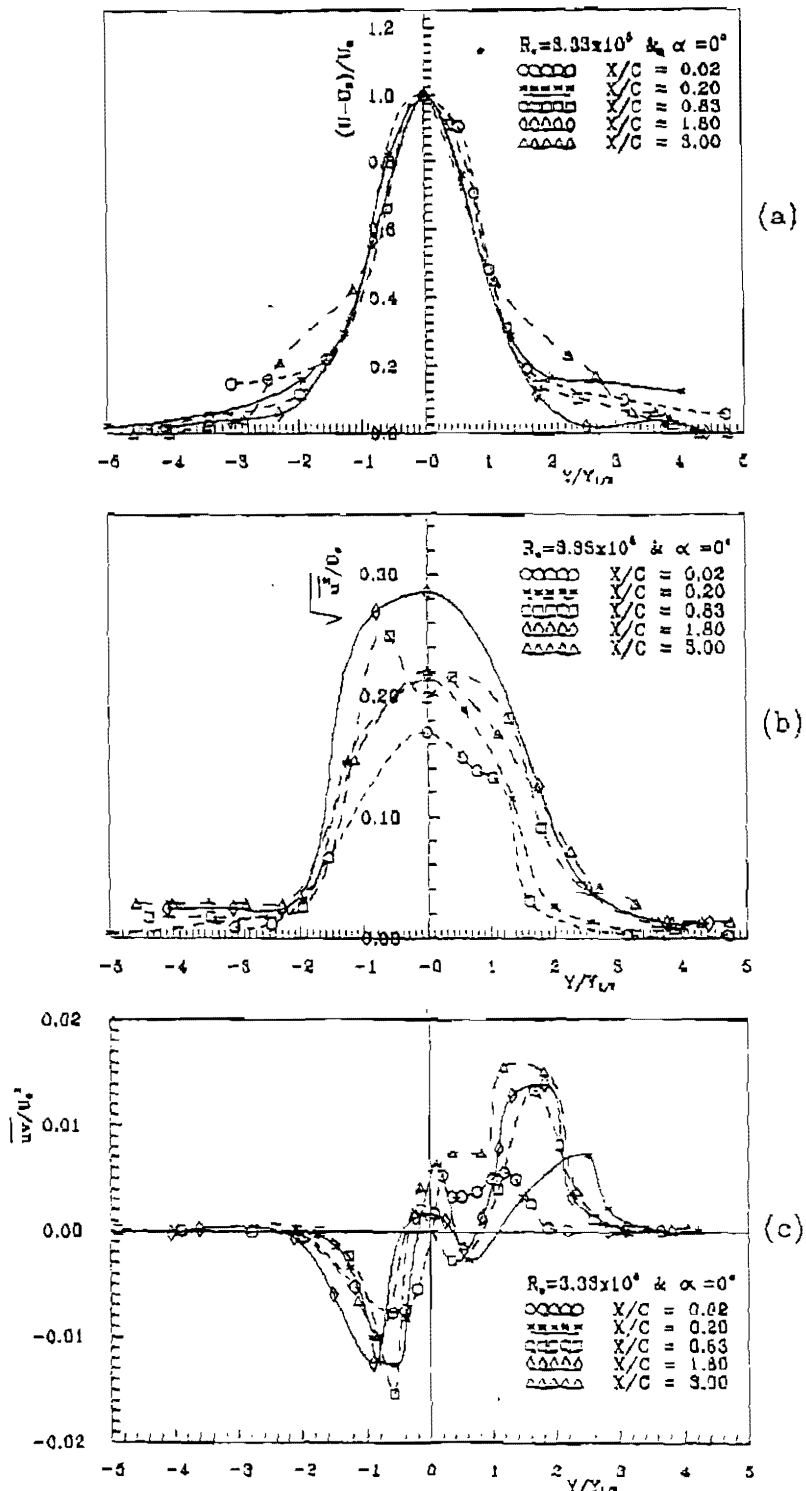

Figure (10) Dimensionless wake parameters for NACA 0012.
a) Longitudinal mean velocity. b) Longitudinal fluctuating velocity.
c) Shear stress

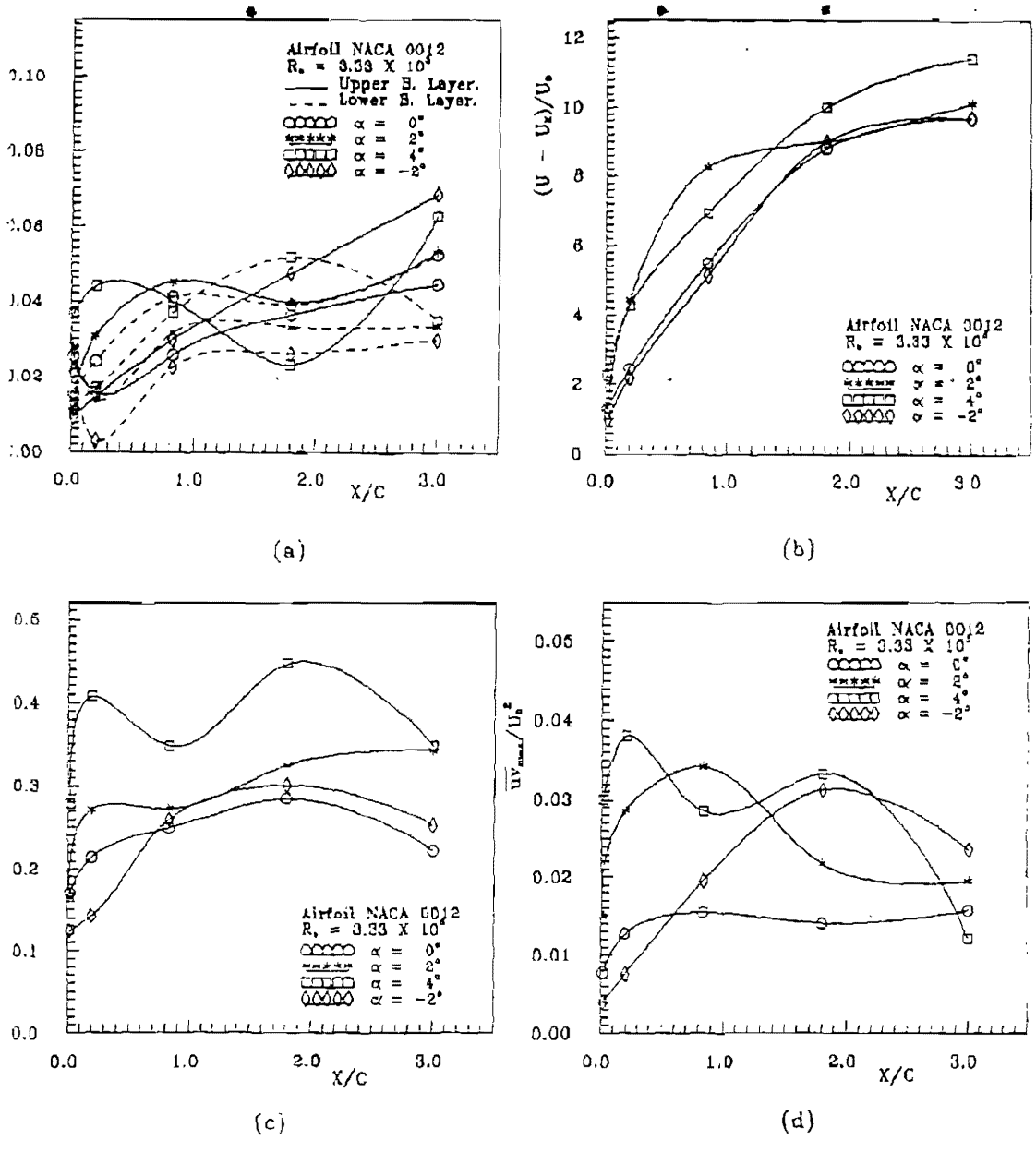

Figure(11) Variation of wake characteristics with downstream distance for NACA 0012
a) Wake half-width. b) Minimum longitudnal mean velocity.
c) Maximum longit. fluctuating velocity. d) Shear stress.

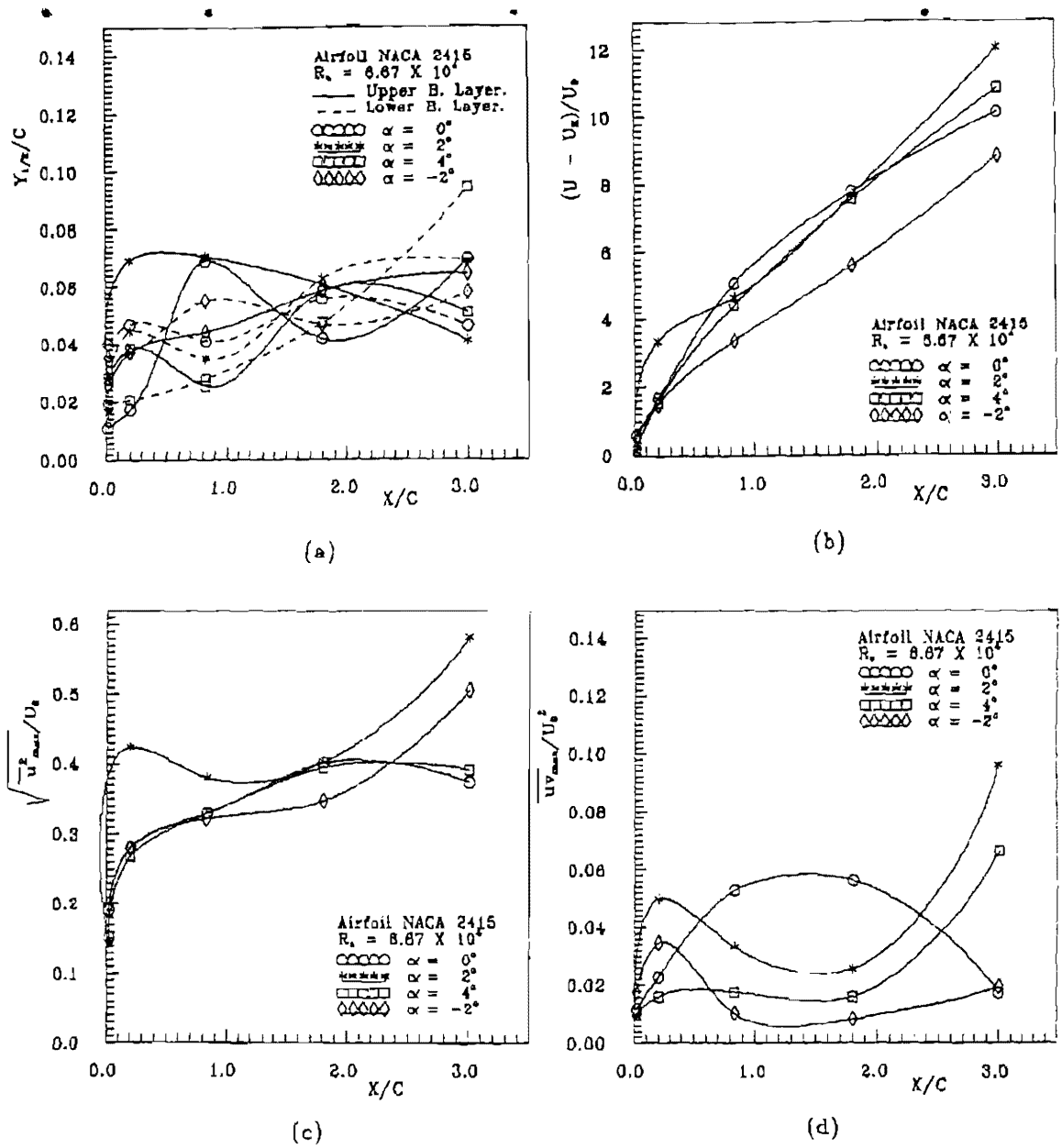

Figure(12) Variation of wake characteristics with downstream distance for NACA 2415.
a) Wake half-width. b) Minimum longitudnal mean velocity.
c) Maximum longit. fluctuating velocity. d) Shear stress.

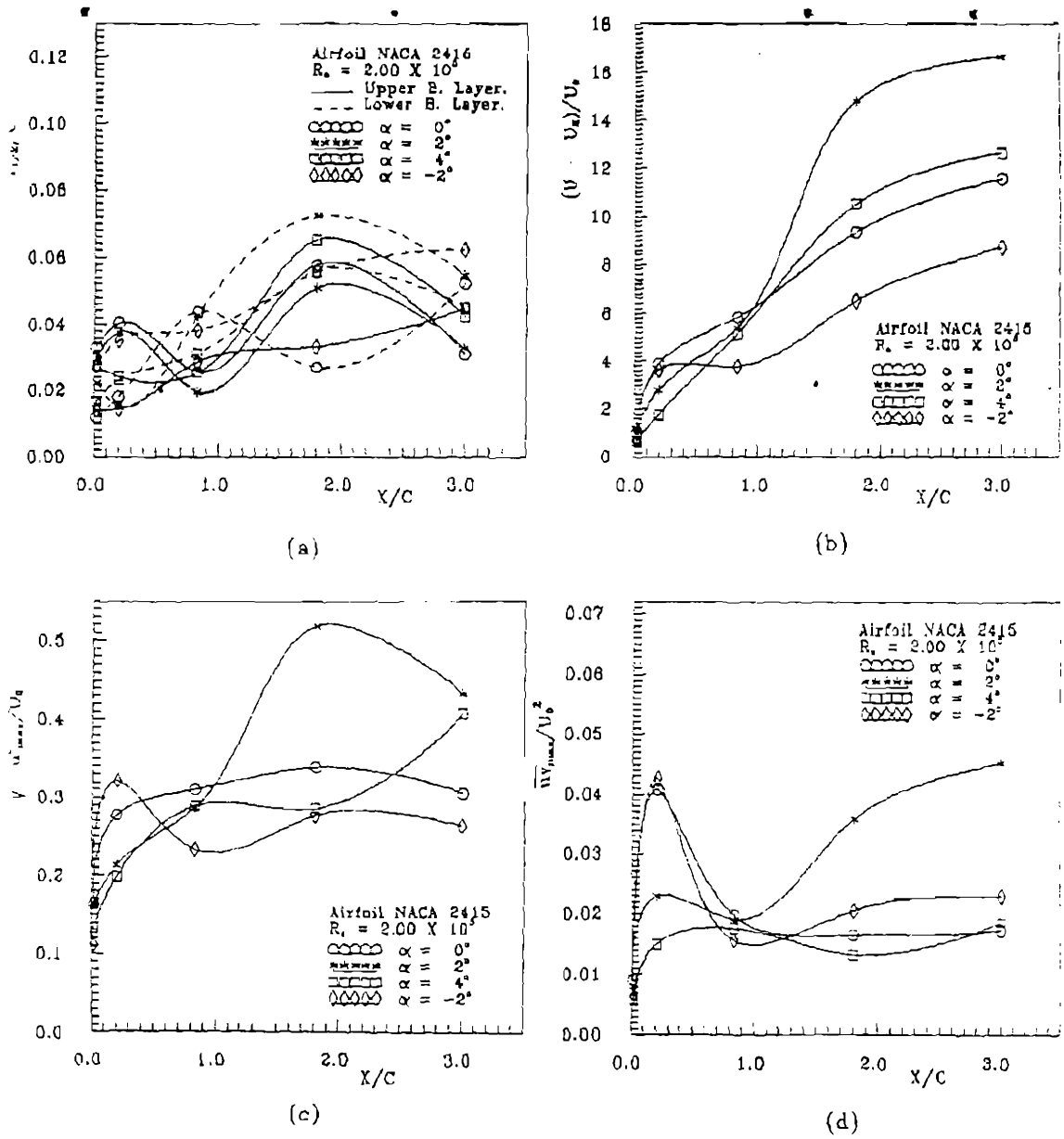

Figure(13) Variation of wake characteristics with downstream distance for NACA 2415.
a) Wake half-width. b) Minimum longitudnal mean velocity.
c) Maximum longit. fluctuating velocity. d) Shear stress.

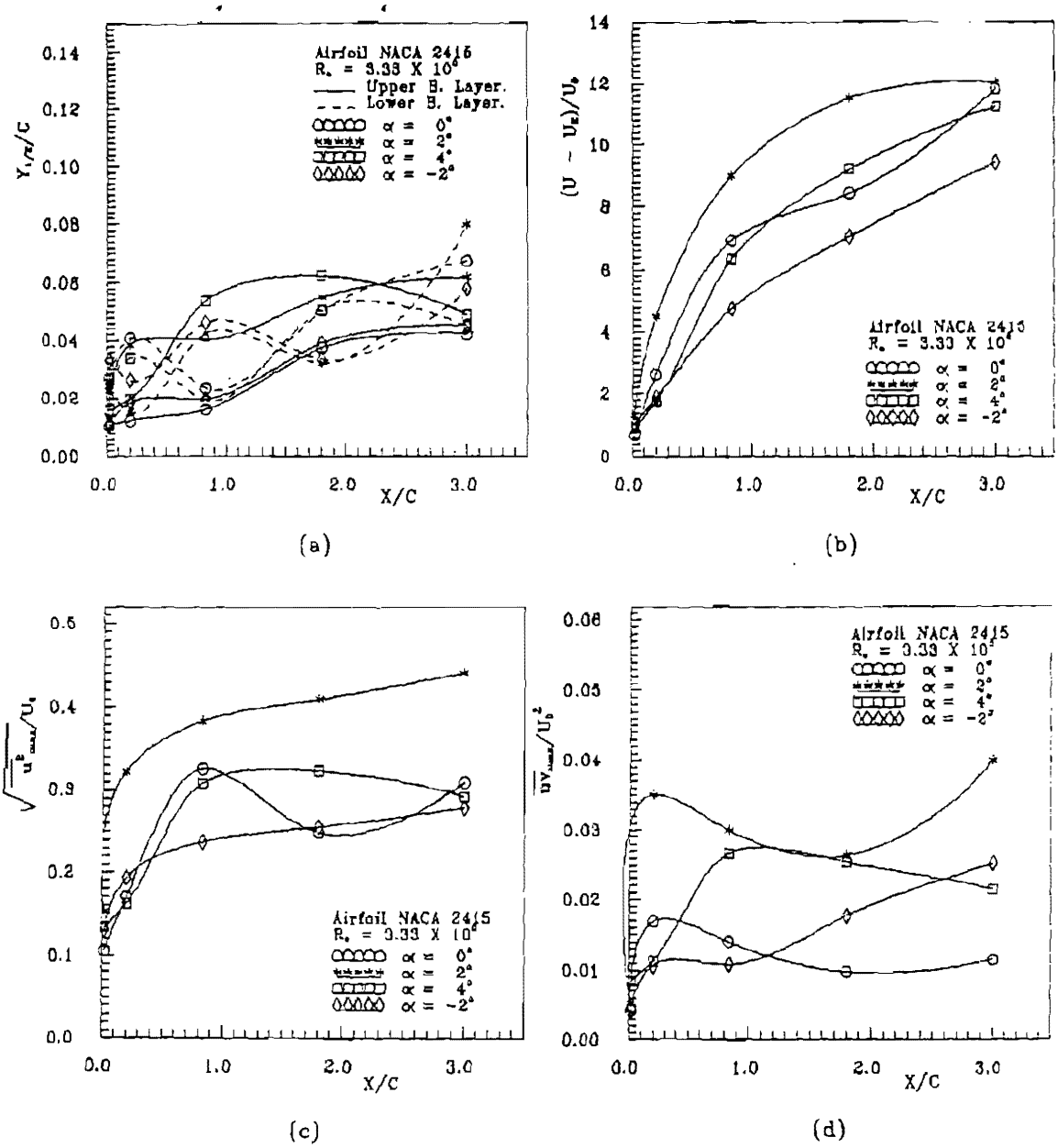

Figure(14) Variation of wake characteristics with downstream distance for NACA 2415.
a) Wake half-width. b) Minimum longitudnal mean velocity.
c) Maximum longit. fluctuating velocity. d) Shear stress.

main streamlines come together, and the length of the wake is limited. The results indicated this phenomena, figure (3-a), since the minimum mean velocity increases rapidly.

When Reynolds number R_e increases, the eddies elongate and a periodic oscillation of the wake is observed. Then at a certain limiting value of Reynolds number ($R_e = 2x10^5$), the eddies break of from each side of the airfoil alternately and are washed downstream then the wake becomes much wider. This limiting value of Reynolds number R_e depends on the turbulence of the oncoming flow, on the shape of the airfoil section and the angle of attack, figure (15-b).

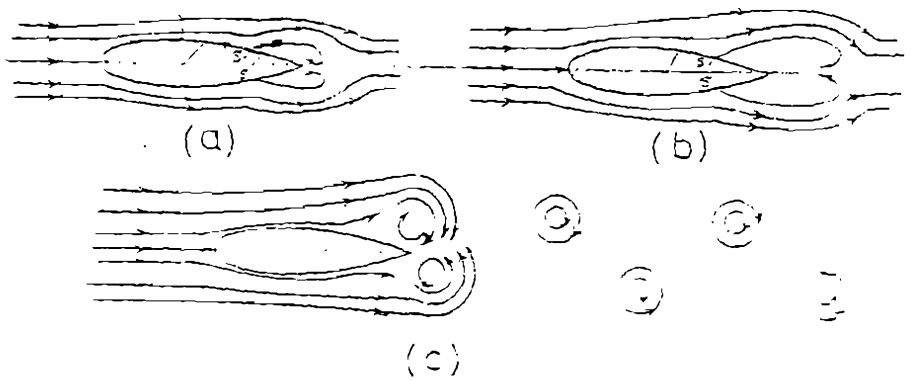

Figure (15) Development of wake behind airfoil section

In higher ranges of Reynolds number (R_e = 3.33 x 10^5) eddies are continuously shed alternately from the two sides of the airfoil section and, as a result, they form two rows of vortices in its wake, the center of a vortex in one row being opposite the point midway between the centers of consecutive vortices in the other row, figure (15-c). This arrangement of vortices is known as a vortex street. This phenomena effects the shape of the shear stress profiles, figure (8-c), particularly their effect is clear in the first four downstream sections. The energy of the vortices is ultimately consumed by viscosity, and beyond a certain distance from the airfoil the regular pattern disappears. This is shown in figure (8-c) at the last downstream distance (x/c = 3.0).

5.3.EFFECT OF ANGLE OF ATTACK:

Increasing the angle of attack α generates circulation round the airfoil, and hence the lift force increase. The adverse pressure gradient along the rear part of the upper surface (lower pressure surface) is intensified. This intensification grows until a particular value of the angle of attack then the boundary layer

separates from the upper surface and a turbulent wake is formed. The results show that at fairly small angle of attacks ($\alpha = 0^{o}$ and 2^{o}), the position of separation may be quite close to the trailing (rear) edge of the airfoil. As the angle of attack increases further ($\alpha = 4^{o}$), the position of separation moves forward and the wake becomes wider.

6-CONCLUSIONS:

The experimental study carried out on the near wake flow behind two airfoil sections (NACA 0012 and 2415) revealed that the wake size and length depend on the airfoil geometry, Reynolds number of the flow and the angle of attack of the airfoil section. It also indicated that there is no similarity between the dimensionless velocity profiles, turbulence intensity and the dimensionless shear stress profiles in this region of the flow. The turbulence intensity $\sqrt{\overline{u^2}_{max}} / U_o$ increases with the increase of Reynolds number while it decreases with the increase of the angle of attack. The dimensionless shear stress ($\overline{uv} / U^2_o$) decreases with the increase of the angle of attack while it decreases with the increase of Reynolds number. The results can be used to check the accuracy of the existing turbulence models to predict this kind of flow.

7.NOMENCLATURE:

c	Cord length of airfoil.
C_1, C_2	Hot wire linearizer constants.
e_L	Fluctuating linearizer voltage.
E_L	Mean linearizer voltage.
R_e	Reynolds number ($R_e = cU / \upsilon$)
u	Longitudinal turbulence fluctuation component.
u_{max}	Maximum longitudinal turbulence fluctuation component.
U	External mean velocity.
U_E	Longitudinal mean velocity.
U_{min}	Minimum longitudinal mean velocity.
U_o	Excess velocity ($U_o = U_E - U_{min}$)
v	Transverse turbulence fluctuation component.
V	Transverse mean velocity.
$\overline{uv}$	Shear stress.
$\overline{uv}_{max}$	Maximum shear stress
x, y	Longitudinal and transverse dimensional co-ordinates
$Y_{1/2}$	Wake half-width.
μ	Fluid dynamic viscosity.
υ	Fluid kinematic viscosity.
α	Angle of attack.

8.REFERENCES:

1- Fukano, T. & Fukuhara, M. & Matsuo, S. and Hayashi, H., "Experimental Study on the Characteristics of the Near Wake of a Rotating Flat Plate (2nd Report, Influence of the Tip Clearance Flow with a Small Attack Angle)", Transactions of the JSME, Part B, V. 57, n 535, PP 891-897, March 1991.

2- Fukano, T. & Hayashi, H. & Kataoka, S. & Hara, Y. and Fukuhara, M., "Experimental Study on the Characteristics of the Near Wake of a Rotating Flat Plate (1st Report, Influence of the Tip Clearance Flow with a Large Attack Angle)", Transactions of the JSME, Part B, V. 55, n 509, PP 56-61, Jan. 1989.

3-Hanson, D.B. and Patrick, W.P., "Investigation of the Near Wake of a profan", Journal of aircraft, V. 27, N. 6, PP 536-542, Jan. 1990.

4-Sirka, V.P. & Daujotas, P.M. and Zukauskas, A.A., "Characteristics of Near Wake of a Cylinder Crossflow", Fluid Mechanics, Soviet Research, V.18, N.4, PP 13-22, Jul.-Aug. 1989.

5-Andreopoulos, J. and Bradshow, P., "Measurements of Interacting Turbulent Shear Layer in the Near Wake of a Flat Plate", Journal of Fluid Mechanics, V. 100, PP 639-668, 1980.

6-Ramaprian, B.R. & Patel, V.C. and Sastry, M.S., "Symmetric Turbulent Wake of a Flat Plate", AIAA journal, V. 20, PP 1228-1235, 1982.

7-Staubli, T. and Rockwell, D., "Pressure Fluctuations on an Oscillating Trailing Edge", Journal of Fluid Mech., V. 203, PP 307-346, Jan. 1989.

8-Thompson, B.E. and Whitelaw, J.H., "Flow Around Airfoils with Blunt, Round and Sharp Trailing Edges", Journal of Aircraft, V. 25, N. 4, PP 334-342, Apr. 1988.

9-Bradshaw, P., "An Introduction to Turbulence and its Measurements", Pergamon Press, Oxford, U. K., 1971.

10-Mohamed, M. S. "Experimental and theoretical investigations of turbulent jets in co-flowing streams", Ph. D. Thesis, Mechanical Engineering Department, UMIST, U.K., October (1987).